A probe for investigating the effects of temperature, strain, and magnetic field on transport critical currents in superconducting wires and tapes

Cite as: Review of Scientific Instruments **71**, 4521 (2000); https://doi.org/10.1063/1.1324734
Submitted: 06 October 1999 . Accepted: 18 September 2000 . Published Online: 30 November 2000

Najib Cheggour, and Damian P. Hampshire

A probe for investigating the effects of temperature, strain, and magnetic field on transport critical currents in superconducting wires and tapes

Najib Cheggour and Damian P. Hampshire[a)]
Superconductivity Group, Department of Physics, University of Durham, Durham DH1 3LE, United Kingdom

(Received 6 October 1999; accepted for publication 18 September 2000)

A variable-temperature probe has been developed to study the effect of strain on the transport properties of superconducting wires and tapes in high magnetic fields. The strain is applied to the wire by soldering it to a thick coiled spring and twisting one end of the spring with respect to the other. Strain can be applied reversibly from -0.7% to $+0.7\%$. Measurements can be performed either in (pumped) cryogen or under vacuum. When immersed in liquid helium at 4.2 K, the probe can carry at least 200 A. From 6 to 16 K, with thin (low-loss) current leads the temperature of the sample is stable to ± 45 mK for currents around 15 A, and to ± 100 mK for currents around 25 A. With thick current leads, ± 10 mK stability is achieved for currents up to 85 A. Full details of the probe design are described. Results obtained for a bronze processed niobium–tin multifilamentary wire are presented. © *2000 American Institute of Physics.* [S0034-6748(00)04112-5]

I. INTRODUCTION

The technology of superconducting magnets requires accurate transport critical current density (J_c) data for the conductor in use under the operating conditions. In addition to the effect of magnetic field (B) and temperature (T), the strain state of superconducting wires and tapes also has an important influence on the J_c properties.[1] Both the differential thermal contraction between the components of the magnet during the cooldown to the operating temperature and the Lorentz force produced by the self-field put the conductor under strain (ε). To accurately predict the magnet's performance, it is therefore crucial to determine the J_c tolerance of the conductor to strain. For this purpose, different probes have been developed by various authors to perform transport $J_c(B,\varepsilon)$ measurements in liquid cryogen.[1–6] This effort has allowed the characterization of low temperature (low-T_c) practical superconductors[1–4,6–8] as well as the high-temperature (high-T_c) superconductors.[4–6,9,10]

Most probes currently constructed for transport $J_c(B,\varepsilon)$ measurements are restricted to temperatures of (pumped) liquid cryogens. In general, they are used in solenoid magnets and designed to test short samples such that the sample is perpendicular to the direction of the magnetic field. A disadvantage in performing transport measurements on short samples is that the current contacts are close to the region between the voltage taps. Depending on the particular superconducting composite under investigation, the region where the current transfers into the superconductor can cause a current-transfer voltage to develop. In this case, corrections to the data are required to extract approximate J_c values from current-voltage ($I-V$) traces.[11,12] To minimize this problem, sufficient room between current contacts and voltage taps has to be allowed, which requires the use of large cold-bore solenoids and restricts the region between the voltage taps to only a few millimeters. Alternatively, strain probes to test long straight samples can be constructed for use in split-coil magnets, but the maximum field these magnets can provide is rather limited. The design proposed by Walters, Davidson, and Tuck presents an interesting solution to these stringent limitations.[3] In this technique, the strain is applied to the wire by soldering it onto a spring and twisting one end of the spring with respect to the other. Primary advantages of this technique are that compressive as well as tensile strain can in principle be applied to the wire. The spring supports the sample mechanically against the Lorentz force produced during the measurements and long samples can be measured in standard high-field solenoid magnets.

Advances in cryocooler technology have offered the possibility of constructing cryogen-free high magnetic field systems. Very recent reports clearly demonstrate the feasibility and reliability of such systems, for both high-T_c[13] and low-T_c[14] superconductors. For an optimum design of cryocooled magnets, comprehensive $J_c(B,T,\varepsilon)$ data are required. To date, variable-temperature $J_c(B,\varepsilon)$ measurements performed are limited to the temperatures of pumped cryogens[6] or carried out on samples with very low critical currents.[15] Recently, $J_c(B,\varepsilon)$ measurements of niobium–tin (Nb_3Sn) superconducting wires performed at 6.5 K have been reported, using a probe designed for short samples.[16] We have built a probe for measuring variable-temperature and variable-strain transport J_c on long specimens in high magnetic fields, throughout a wide temperature and strain range.

In this article, we present a detailed account of the design of the probe. The strain is applied using the spring technique.[3] The titanium alloy proposed by Walters and coworkers for fabricating the spring is replaced by a copper–beryllium alloy which is easy to solder to. This makes it possible to apply both compressive and tensile strain, reversibly between -0.7% and $+0.7\%$. The probe operates either under vacuum or in (pumped) cryogen. The probe is designed to operate in magnets with a cold bore as small as 39

a)Electronic mail: d.p.hampshire@durham.ac.uk

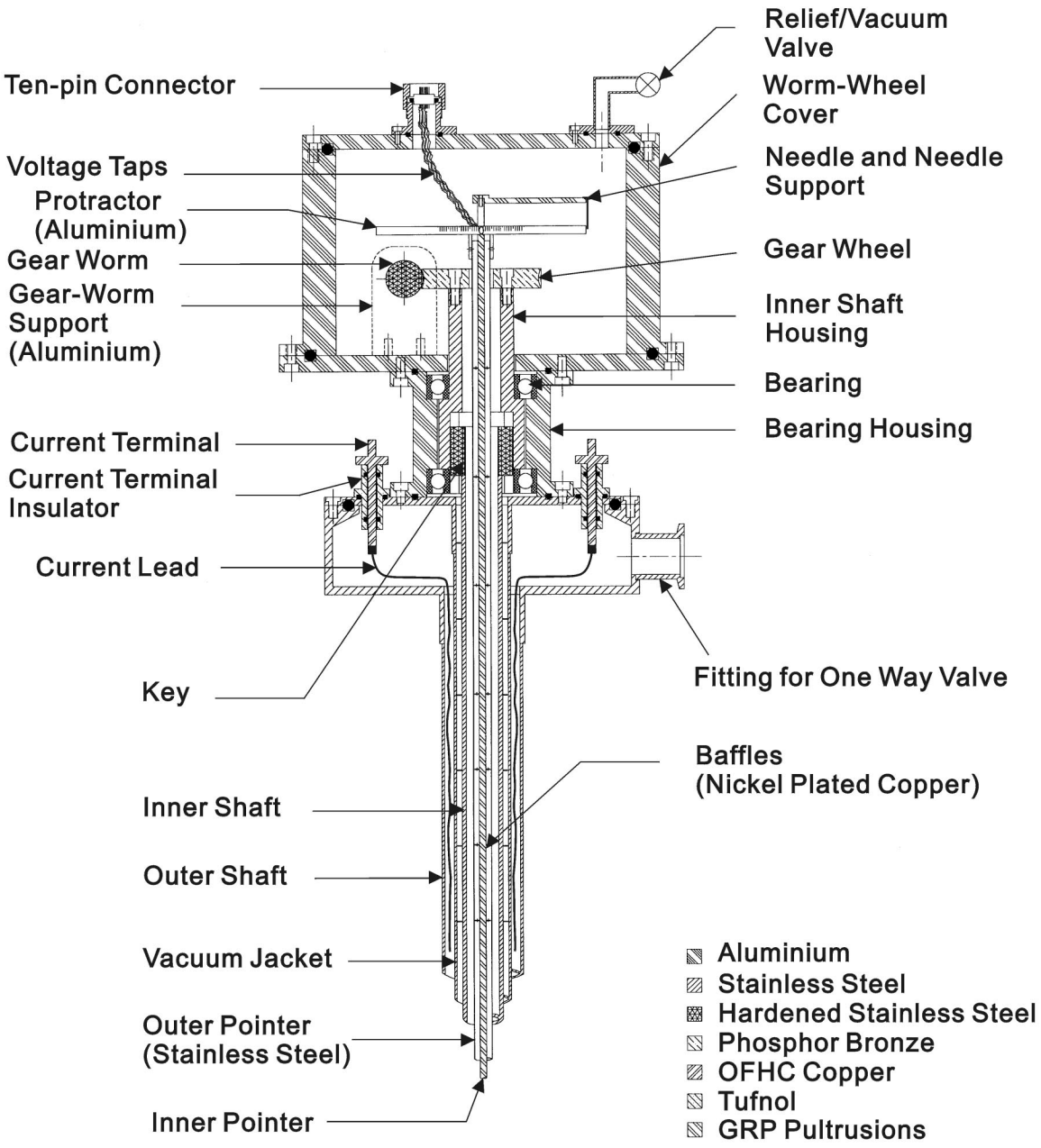

FIG. 1. Diagram of the top part of the probe designed for $J_c(B,T,\varepsilon)$ measurements on superconducting wires and tapes.

mm. Due to the high endurance to fatigue of copper–beryllium alloy, it is also possible to use the probe for investigating the effect of multiple cyclic loading on transport properties of superconducting wires and tapes. We present $J_c(B,T,\varepsilon)$ measurements carried out on a bronze processed Nb_3Sn multifilamentary wire, at the temperatures of 4.2, 6.5, 9, and 13.8 K, as a function of magnetic field up to 15 T, for a wide strain window from -0.7% to $+0.7\%$. The reversibility of J_c with strain cycles is also examined. Data are presented that demonstrate the accuracy and reliability of the probe.

II. DESIGN OF THE PROBE

A. Description

The top and bottom parts of the probe are presented in Figs. 1 and 2, respectively. The probe can be inserted into magnetic field systems having a cold bore of 39 mm in diameter or higher. Particular attention was given to minimize the overall weight of the apparatus. For this purpose, aluminum was used to fabricate most of the parts which are not under mechanical stress during the experiments. In contrast, the pieces that sustain the stress were made of stainless steel, phosphor bronze or a copper–beryllium alloy. The maximum stresses these pieces are subjected to were estimated and their size optimized accordingly.

1. Application of strain

The principle of applying strain to the sample follows the design developed by Walters, Davidson, and Tuck.[3] The superconducting wire or tape to be investigated is soldered to a thick coiled spring. The spring we have designed is made of the 2% beryllium doped copper alloy (alloy 25). It is attached at its top end to a stainless steel tube (inner shaft)

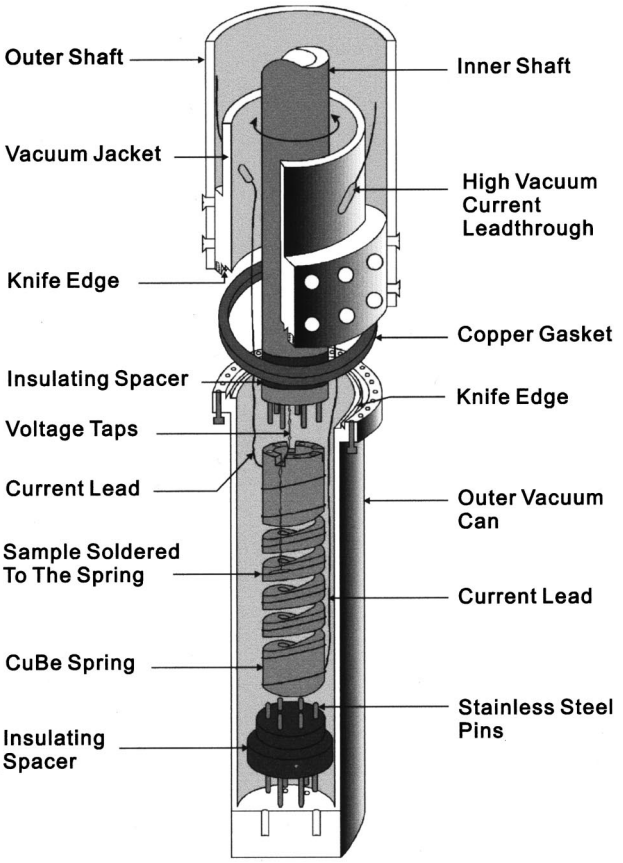

FIG. 2. Schematic of the bottom part of the probe designed for $J_c(B,T,\varepsilon)$ measurements on superconducting wires and tapes. For measurements at temperatures of liquid cryogens, the outer vacuum can is replaced by a can with holes at the bottom.

and has its bottom end locked by the outer (vacuum) can (Fig. 2). The latter, also made of stainless steel, is firmly fastened to the bottom of the probe, while the inner shaft is connected at its top end to a worm-wheel gear system located at the head of the probe (Fig. 1). The spring is electrically insulated from the inner shaft and the outer can by tufnol spacers and the attachments are made using stainless steel pins (Fig. 2). The gear system is hand operated. Turning the gear worm rotates the inner shaft, which transmits a torque to the spring. This generates an angular displacement between the spring ends. Depending on the sense of rotation, the sample is put under either a tensile or a compressive strain.

To measure the angle of twist applied to the spring, two pointers are attached to the spring ends.[3] The top end of the spring is connected to a thin-walled long stainless steel tube (outer pointer), while the bottom end is attached to a long rod (inner pointer) via the thermometry block located inside the spring (thermometry block and pointers not shown in Fig. 2). The rod is 4 mm in diameter and is made of a plastic (GRP Pultrusions) of high flexural strength. Both pointers are located inside the inner shaft and emerge at the head of the probe (Fig. 1). A needle and needle support are attached to the inner pointer. A disk-shaped protractor, made of aluminum, is fastened to the outer pointer. When a torque is applied, the position of the needle relative to the protractor allows the measurement of the angle of rotation of the outer pointer with respect to the inner one. From the reading of the angle of twist (θ), the value of strain applied to the sample can be derived.[3] The exact relationship between ε and θ is determined by calibrating the spring using standard strain gauges (cf. Sec. III A).

The head of the probe is encapsulated by a worm-wheel cover made of aluminum. To allow the reading of the angle θ, the cover contains three windows cut out at about an angle of 120° from each other (windows not shown in Fig. 1). The windows are closed by fastening to the cover thin disks of Perspex. A fourth port houses a rotary vacuum seal for the gear worm. The top of the cover contains a vacuum valve to connect the apparatus to the pump. It also accommodates three ten-pin connectors for the instrumentation leads. All the instrumentation leads run through protective sleeves down to the thermometry block and the spring, and are attached with Mylar tape to the inner pointer. Use of O rings ensures that the room-temperature part of the probe is leak tight.

2. Vacuum and high-current leads

The variable-temperature transport J_c measurements above the temperature of liquid helium are performed under vacuum to insure good temperature control.[17] For this purpose, the spring is located in a vacuum chamber encapsulated by a demountable outer can at the bottom end of the probe. The vacuum chamber extends to the head of the apparatus by means of a stainless steel tube (vacuum jacket) which serves as the vacuum pumping line. The vacuum jacket and the outer can are attached by a knife edge vacuum joint (Fig. 2). The vacuum seal is formed by compressing a copper gasket between the two knife edges. The seal transmits the torque to the spring and, therefore, must be mechanically strong enough not to leak when a torque is applied. For this reason, the technique of knife edges and a copper gasket was chosen to attach the vacuum can to the probe, instead of solder or vacuum grease used in the $J_c(B,T)$ probes previously constructed in our group.[17] To perform the measurements in (pumped) liquid cryogen, a second outer can is used, which does not contain a knife edge and has six holes at its bottom end to allow liquid cryogen to fill up the space around the sample.

The (low-loss) current leads are soldered to the current terminals at the top of the probe and extend down to the sample. The leads enter the vacuum chamber through low temperature, high vacuum current leadthroughs.[18] Two holes are made near the bottom of the vacuum jacket to accommodate the leadthroughs. The latter consist of short brass tubes, hard-soldered to the vacuum jacket (Fig. 2). They each accommodate 1-mm-diam copper wire and are sealed using Stycast epoxy. Between the leadthroughs and the current terminals, the size of the current leads gradually changes to minimize the static helium boil-off. At the current terminals, each lead consists of two copper wires 1.2 mm in diameter and two CuNi/NbTi superconducting wires 0.3 mm in diameter. Below the leadthroughs, each current lead includes one copper wire 1 mm in diameter and one CuNi/NbTi wire 0.3 mm in diameter. A stainless steel tube (outer shaft) slides over the vacuum jacket and is firmly fastened to it (Figs. 1 and 2). The outer shaft reinforces the vacuum jacket to sus-

TABLE I. Mechanical properties of CuBe and titanium alloys.

	CuBe (alloy 25)		Titanium (318)	
	293 K	4.2 K	293 K	4.2 K
Young modulus E (GPa)[a,b]	119	132	105	⋯
Proportional limit of elasticity (%)[a,b,c]	0.9	1.0	0.9	⋯
Fatigue strength (MPa), in reversed bending at 10^8 cycles (293 K)[c]	315		⋯	

[a]Reference 19.
[b]Reference 20.
[c]Reference 21.

TABLE II. Thermal conductivity (W/mK).

T (K)	Copper[b]	Brass Yellow[b]	CuBe Alloy 25[a]	Titanium 318[c]	AISI 304[b]	Solder 60Sn/40Pb[b]
293	401	126	105	7.5	15	50[d]
77	584	39	37	2.7	8	51
20	10 800	12	11	1.7	2	55
4.2	16 200	2.3	2	1.5	0.3	16

[a]Reference 19.
[b]Reference 24.
[c]Reference 25.
[d]Solder 50Sn/50Pb.

tain the torque. It also protects the current leads and fits the neck of the magnet cryostat.

The helium gas produced when an electric current flows, escapes through the one-way valve (Fig. 1) and cools the current leads. Currents up to about 160 A have been measured when the sample is immersed in liquid helium. In vacuum, the heat generated by the leads is compensated for by a feedback circuit which reduces the power dissipated by the heater located around the spring. The maximum current that can accurately be measured depends on the temperature as well as the sample under investigation. From 6 to 20 K, the probe can accurately measure currents typically up to 25 A. We have recently increased the maximum current to ~ 85 A by using thick current leads at the expense of higher static helium boil-off (cf. Sec. VIII).

3. Thermometry

The temperature of the sample is controlled by a Rh-Fe thermometer and a field-independent capacitance thermometer, both placed inside the thermometry block. The thermometry block is situated inside the spring, but electrically insulated from it by means of a tufnol spacer. A gap of 1 mm is allowed between the thermometry block and the inner surface of the spring. The thermometry block is made of high thermal conductivity oxygen-free high-conductivity (OFHC) copper. In zero field and zero strain the temperature of the sample was accurately measured using a calibrated Cernox thermometer attached directly to the outer surface of the spring, next to the sample.

To vary the temperature of the sample, a 55 Ω heater is placed around the spring (heater not shown in Fig. 2). It consists of a constantan wire mounted on a thin-walled cylindrical support, concentric with the spring. This support is made of OFHC copper to improve the homogeneity of temperature in the sample space. In order to cut radiation, approximately ten layers of aluminized Mylar superinsulation are wrapped around the heater support. For a similar purpose, baffles made of nickel-plated copper are attached to the inner pointer and the inner shaft (Fig. 1).

B. Spring

1. Material for the spring fabrication

The material of the spring has to be properly selected to meet particular requirements concerning mechanical behavior, solderability, as well as thermal and electrical properties.

It is preferable that the proportional limit of elasticity of the spring is higher than the maximum strain needed to investigate the sample. This condition is necessary to prevent the spring from plastically yielding, and to allow accurate study of the J_c reversibility with strain. Moreover, the high elasticity of the spring ensures reversibility and reproducibility of the spring calibration, and has the advantage that, once the spring is calibrated, a strain gauge does not need to be attached to the sample during each experiment. Besides its high elasticity, the material should also have good solderability in order to attach the sample to the spring. This property is particularly important in facilitating the application of compressive strain.

Few materials have sufficiently high proportional limit of elasticity to make them suitable for the spring fabrication. Walters, Davidson, and Tuck[3] proposed a 318 titanium alloy which has a proportional limit of elasticity of 0.9% at room temperature (Table I[19–21]). However, this material has a poor solderability. We have chosen a 2% doped beryllium copper alloy (alloy 25). This material, cold worked and precipitate hardened at 315 °C for 2 h (temper TH04), has a proportional limit of elasticity of about 0.9% at room temperature, and about 1% at 4.2 K (Table I). The good solderability of this alloy provides a significant advantage over the titanium alloy. However, the temperature for soldering must be kept significantly below the precipitate-hardening temperature in order that the spring does not undergo changes in its elastic properties.[22] Standard Pb/Sn soft solders are convenient for this purpose.

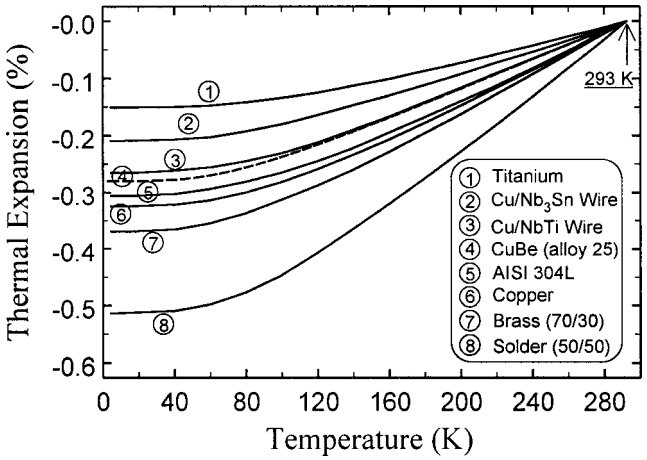

FIG. 3. Thermal expansion of CuBe alloy, compared to some metals (titanium, copper), alloys (AISI 304L, brass 70/30, solder 50/50), and superconducting composites (Cu/Nb_3Sn, Cu/NbTi) (see Refs. 26 and 27). The data for Cu/Nb_3Sn were obtained on a conductor with a tungsten core (see Ref. 27).

TABLE III. Electrical resistivity (nΩ·m).

T (K)	Copper[c]	Brass Yellow[c]	CuBe Alloy 25[a]	Titanium 318[b]	AISI 304[c]	Solder 50Sn/50Pb[c]
293	16.8	64	65	482	720	150
77	2.1	⋯	42	⋯	⋯	⋯
4.2	0.02	⋯	40	⋯	⋯	⋯

[a]Reference 19.
[b]Reference 20.
[c]Reference 24.

Furthermore, when a strain is applied, the Poisson ratio of the spring material may influence the transverse strain on the sample. To determine the precise strain state of the sample, the Poisson ratio of the spring material and the composite as well as their thermal expansions have to be known.[4,23] The Poisson ratio of CuBe will be addressed in Sec. III A.

Thermal properties of the spring material have to be adequate. The thermal conductivity of the material needs to be high enough to ensure uniform temperature along the length of the sample, and a good thermal contact between the sample and the thermometry block. In addition, there should be a good matching of the thermal expansion between the spring material and the sample in order to prevent thermal strain on the sample during the cooling from the soldering temperature to the temperature of the measurements.

In Table II,[19,24,25] thermal conductivity data of CuBe are presented and compared to some other materials. CuBe has better thermal conductivity than either 318 titanium alloy or stainless steel 304, and therefore is a better choice to fulfill the requirements discussed above. In Fig. 3, the thermal expansion of some metals, alloys and superconducting composites are presented for comparison.[26,27] We have calculated the thermal expansion of CuBe from thermal expansion coefficient data.[19] It must be noted that the thermal expansion data shown for NbTi and Nb_3Sn superconducting wires are indicative only. The thermal expansion may vary depending on the exact construction of the conductor considered. Note that for Cu/Nb_3Sn conductors, the only thermal expansion versus temperature data available are for a conductor with a tungsten core which reduces the magnitude of the overall conductor's thermal expansion.[27] Thermal expansion values have also been reported for various conventional Cu/Nb_3Sn conductors for 77 K with respect to room temperature and are found to be -0.26% to -0.28%.[28,29] The equivalent thermal expansion of CuBe alloy at 77 K is -0.26%. We conclude that the thermal expansion of CuBe is well matched to NbTi and Nb_3Sn composites and better than either stainless steel or brass.[30]

To ensure that the current flows through the superconductor, the electrical resistivity of the spring should be relatively high. This is particularly important for samples that have small cross sections compared to the section of the spring. The high resistivity of the shunt prevents broadening of the $I-V$ traces which affects evaluating J_c values intrinsic to the composite. Electrical resistivity data for the CuBe alloy are presented in Table III.[19,20,24] As will be confirmed by the data in Sec. VII, the electrical resistivity of CuBe is sufficiently high.

The endurance to fatigue of CuBe alloy is quite high (Table I). This property offers the additional possibility of using the probe to examine the effect of fatigue on the transport properties of wires and tapes.[31–33]

These general considerations convinced us to choose CuBe alloy as the material for the spring. The spring can be machined first and subsequently precipitate hardened but particular precautions have to be taken during the heat treatment in order to maintain the shape of the spring.[34] To avoid this problem, we have machined the spring from a tempered CuBe rod.

2. Spring design

The spring has a rectangular section. When an angular displacement between the ends of the spring is applied, the strain varies throughout the spring section. There is a neutral radius where the material remains unstrained. Above and below the neutral radius, the strain is of opposite sign.[3] In case of pure torque and in the absence of radial compression, the ratio of the strain at the inner and outer radius (R_1 and R_2, respectively) of the middle turns of the spring depends on the ratio $r_0 = R_2/R_1$ as

$$\frac{\epsilon(R_2)}{\epsilon(R_1)} = \frac{\frac{1}{r_0} - 1 + \ln(r_0)}{1 - r_0 + \ln(r_0)}, \tag{1}$$

where this expression is derived from the formulas in Ref. 3. The magnitude of strain at the inner surface of the turns is the highest. As the proportional limit of elasticity (ε_p) of CuBe should not be exceeded at any point in the spring, the condition $\varepsilon(R_1) \leqslant \varepsilon_p$ must be observed.[3] Therefore, the maximum strain recommended (at the outer surface) has to be lower than the proportional limit of elasticity of the spring material. This maximum allowable strain ($\varepsilon_{\max}$) is closer to ε_p as r_0 tends towards 1. Nevertheless, the spring must have enough thickness in order not to compromise its rigidity. Note that there is a transition region at the ends of the spring where the strain at the outer surface is smaller and nonuniform compared to that of the middle turns. To avoid this problem, all the voltage taps for $I-V$ measurements are placed at least half of a turn away from the spring ends.

The inner and outer diameter of the spring are set to $2R_1 = 12.9$ mm and $2R_2 = 22$ mm. This choice takes into account the size constraints imposed by the bore size of our magnet and the thermometry block which is located inside the spring. The thickness of the turns is $h = 4.55$ mm. This spring geometry corresponds to $r_0 = 1.7$ and, therefore, to a maximum strain allowable at 4.2 K of $\pm 0.7\%$. The spring contains four turns in total. The breath of the turns (w) is set to 4.4 mm, sufficiently large to accommodate both wires and tapes (typically 3 mm wide). The pitch from turn to turn is 6.4 mm.

The strain window from -0.7% to $+0.7\%$ is generally sufficient to investigate most superconducting wires and tapes within their reversible regime and beyond.[8,9,35] There are a few exceptions, like NbN wires, which show high tolerance to strain beyond 1%.[8,36] To study such systems, one can change the rectangular section of the spring to a T section as proposed by Walters and co-workers,[3] or operate the

TABLE IV. Maximum shearing stresses in the shafts.

	Inner diameter d (mm)	Outer diameter D (mm)	Maximum shearing stress τ_{max} (MPa)
Inner shaft	20	25	8.3
Outer shaft	50	48	4.1
Vacuum jacket	32	35	5.9
Outer can	35	38	5.0

spring beyond its proportional limit of elasticity with the limitations that follow. Appropriate T-section geometry can be used to extend the allowable strain window to $\pm 1\%$ (at 4.2 K) since the magnitude of strain at the inner and outer surface of the turns becomes equal.[3] However for most technological applications, these data are not required since magnets are designed to operate within an intrinsic strain range of about $\pm 0.4\%$ as insulation and epoxy fracture at higher strain.

It is important to estimate the maximum torque (T_{max}) needed to reach the maximum allowable strain at the outer surface of the spring turns. This facilitates the optimization of the size of the shafts and the worm-wheel gear system. Neglecting the pitch angle, T_{max} for a rectangular-section spring can be expressed as

$$T_{max} = \tfrac{1}{6}\sigma_{max} w h^2, \tag{2}$$

where $\sigma_{max} = E\varepsilon_{max}$ (E: Young modulus) is the stress level which generates a strain of $\pm 0.7\%$ at the outer surface of the spring turns. For the spring designed, T_{max} is about 15 Nm.

C. Shafts and gear system

The torque is applied to the spring by the inner and outer shafts, the outer can and the vacuum jacket. The dimensions of these tubes need to be properly chosen to ensure they are large enough to provide sufficient strength, and small enough to minimize the overall weight of the probe. Optimizing the tube size also helps to minimize the thermal head leak from room temperature.

Consider a tube having an inner diameter d and outer diameter D, subjected to a torque T_{max} about its longitudinal axis. The maximum shearing stress τ_{max} occurs at the external surface of the tube and is given by[37]

$$\tau_{max} = \frac{T_{max}}{\frac{\pi}{16}\left(\frac{D^4 - d^4}{D}\right)}. \tag{3}$$

To avoid breakage or permanent deformation of the tube, the maximum shearing stress τ_{max} must not exceed the allowable stresses for shafts. The latter is generally taken as 28 MPa.[38] In Table IV, the final dimensions of each tube of the probe are presented as well as the maximum shearing stresses these tubes are subjected to when $T_{max} = 15$ Nm is applied. For these choices of tube, the safety factor is at least 3. Note that the outer shaft could be substantially thinner, but we were limited by the dimensions commercially available for high diameter tubes. Only seamless tubes were used.

The torque is applied to the inner shaft and spring using a commercial worm-wheel gear system. The gear worm is made from hardened stainless steel, while the gear wheel is of phosphor bronze. The system can sustain a torque as high as 30 Nm and, therefore, provides a safety factor of 2. To have a sufficiently high-resolution control on the angle of twist applied to the spring ends and avoid backlash, a gear wheel with a high number of teeth (50) was used.

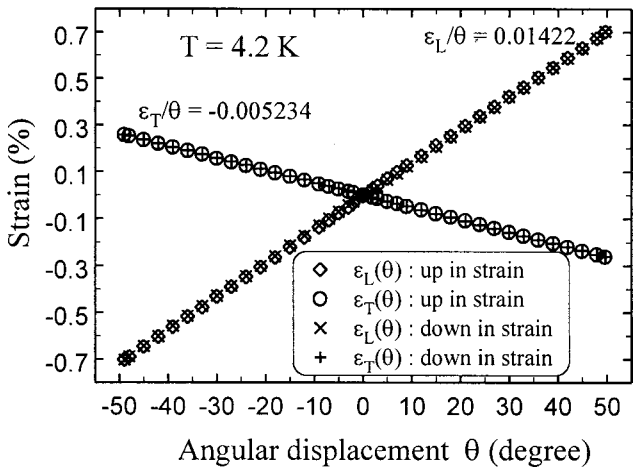

FIG. 4. Calibration of the spring at 4.2 K, which defines the relation between the strain at the outer surface of the spring turns and the angular displacement between the spring ends.

III. MECHANICAL AND THERMOMETRY TESTS

A. Spring calibration

The calibration of the spring was carried out to measure the strain-angle relationship [$\varepsilon(\theta)$]. Nickel–chromium strain gauges were used, which are self-temperature-compensated and match the thermal expansion of beryllium copper alloy. Two strain gauges were glued to the outer surface of one turn in the middle of the spring. One gauge was oriented parallel to the turn and measured the longitudinal strain (ε_L). The second one was mounted adjacent to the first, perpendicularly to the turn to measure the transverse strain (ε_T). The linearity and reversibility of the relationship $\varepsilon(\theta)$ was tested. To check the effect of temperature on $\varepsilon(\theta)$, the calibration was performed at room temperature, 77 and 4.2 K.

The results of the calibration at 4.2 K are presented in Fig. 4. The longitudinal and transverse strain vary linearly as a function of θ for both compressive and tensile strain regimes. As expected, the response is reversible within the strain window from -0.7% to $+0.7\%$. Furthermore, the additional calibrations performed at room temperature and 77 K show that the relationship $\varepsilon(\theta)$ is temperature-independent to better than 2%. The Poisson ratio $-\varepsilon_T/\varepsilon_L$, as measured in this experiment, is about 0.36. The uncertainty in $\Delta\varepsilon/\varepsilon$ is estimated to 2%, although numerical modeling is required to determine the variation in strain throughout the cross-sectional area of the wire.

The weight of the inner shaft loaded on the spring may alter the spring's length and produce an additional strain on the sample. To estimate this strain, the resistance of the strain gauges were measured for both horizontal and vertical positions of the probe. The resistance change between the two positions corresponds to a longitudinal strain less than $1.5\times 10^{-3}\%$. Such a small strain reflects the relatively high stiffness of the spring. Furthermore, when a certain strain is

applied to the spring, no backlash of the worm-wheel gear system can be detected from the reading of the strain gauge. Nevertheless, a lock is available on the probe to ensure that no movement of gear worm occurs during the experiments.

The effect of the Lorentz force on the critical current density was tested. When the direction of the sample current was changed, the J_c measured remained the same. This demonstrates that the sample is well protected against the Lorentz force.

B. Temperature accuracy

A thermal gradient exists between the sample and the two thermometers incorporated in the thermometry block. This gradient is due to the fact that the sample and the thermometry block are not thermally sunk to each other. To accurately measure the temperature of the sample, a calibrated Cernox thermometer is attached to the surface of the spring, adjacent to the sample. This thermometer is electrically insulated from the spring by means of a cigarette paper glued to the outer surface of the spring. Vacuum grease is used to attach the Cernox thermometer to the spring and provides intimate thermal contact between the thermometer and the sample.

The temperature accuracy and calibration is measured at zero strain. The Rh–Fe thermometer is first calibrated with respect to the temperature of the sample at zero strain and zero field. Then the temperature stability during $I-V$ trace acquisitions is tested at different fields. From 6 to 16 K, the temperature of the sample is stable to ± 45 mK for currents around 15 A, and to ± 100 mK for currents around 25 A. Beyond 30 A, the temperature is difficult to control due to the heat generated by the current leads. This limitation has been overcome recently by increasing the size of the leads, at the expense of higher static liquid helium consumption (cf. Sec. VIII).

IV. SAMPLE PREPARATION

The sample must be mounted on the spring very carefully to avoid damaging it before the measurements. Winding a superconducting wire or tape on the spring will strain the conductor as the spring diameter is small. Consequently, the wind and react technique has to be considered. Appropriate heat treatment is also required for ductile materials, like NbTi, in order to release internal stresses in the conductor due to winding. The spring cannot be used as a sample holder during the heat treatments, as the temperature of the spring must be kept far below the precipitate-hardening temperature of beryllium copper alloy.[22] Furthermore, the shape of the spring changes after such heat treatments. Therefore, the sample must be heat treated on a separate mandrel and subsequently transferred onto the spring for the measurements.

The mandrel should be made of a material chemically inert with respect to the conductor. We have used stainless steel mandrels to react Nb_3Sn superconducting wire presented in this article. This choice is also adequate for various conductors such as Chevrel phase, NbTi or Nb_3Al. In the case of high-T_c tapes, alumina may be more appropriate. The mandrel and the spring have the same outer diameter. For superconducting wires with circular sections, standard V-shaped groove with a 60° angle was machined on the mandrel with the same pitch as the spring to accommodate the wire.

To transfer the sample onto the spring, a jig is used to hold the spring and mandrel concentric with each other. By turning a few spires of the sample at the free end of the mandrel, the sample is progressively transferred onto the spring.

The sample preparation is completed by soldering the sample to the spring. The temperature of the soldering is kept below about 240 °C. A 60Sn/40Pb soft solder is used. Because of the mass of the spring, a soldering iron is not sufficient. A heat gun and a hot plate are used instead. A thermocouple is used to preset the temperature of the heat gun. The spring is put vertically on a hot plate and the heat gun used to melt the solder. Phosphoric acid is used as the flux for soldering onto beryllium copper alloy.

Finally, the spring is attached to the probe using the stainless steel pins available at the bottom end of the inner shaft (Fig. 2). Current leads are soldered to the spring ends and voltage taps to the turns. Up to ten twisted pairs of taps are available on the probe. They are fixed along the length of the sample for J_c homogeneity tests. The distance between the voltage taps can be set to cover any sample length up to about 28 cm.

V. PROCEDURE FOR MEASUREMENTS

To perform $J_c(B,\varepsilon)$ measurements at 4.2 K and below, the outer can with clearance holes at the bottom is fastened to the probe. Once the probe has been inserted in the magnet cryostat, the sample is in direct contact with (pumped) helium bath. For measurements above 4.2 K, the outer vacuum can is fastened to the probe. Thus, the copper gasket located between the two knife edges is compressed and the vacuum seal formed. Before inserting the probe into the cryostat, the system is pumped and flushed with helium gas three times. A small amount of He gas is allowed in the vacuum chamber to facilitate cooling down of the probe. Once the system has been inserted into the magnet, the vacuum chamber is pumped to less than 10 Pa and the vacuum valve closed.

The magnetic field is provided by a 15 T superconducting magnet. To measure the $I-V$ traces, a current is supplied to the sample and the voltage generated across the taps measured. Either a commercial 100 A power supply or a 500 A power supply built in house is used for the current. A Keithley 182 digital nanovoltmeter is used to measure the voltage across the sample. For measurements above 4.2 K, the thermometers and heater are monitored by a Lakeshore DRC 91A temperature controller. The heater current is measured using a Keithley 196 digital multimeter. Below 4.2 K, the helium bath is pumped and the pressure is controlled by a commercial pressure controller and throttle valve. Vapor pressure thermometry is used. The $I-V$ acquisition is computer controlled.

The temperature of the sample is set at zero field using the Rh–Fe thermometer, and controlled during the measurements in-field with the field-independent capacitance thermometer. The heater-current is recorded throughout the mea-

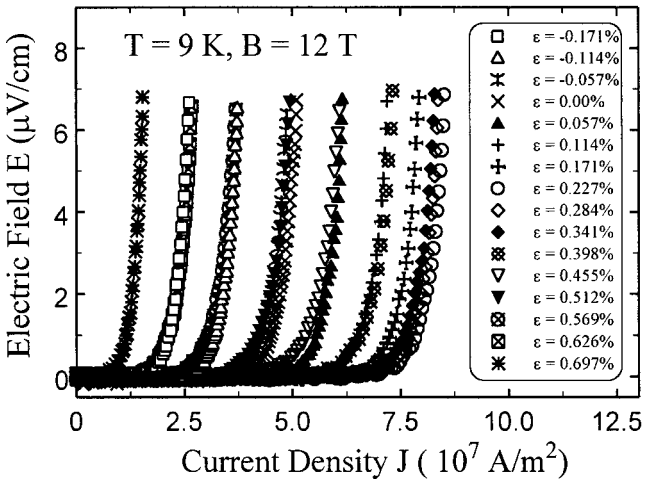

FIG. 5. Typical $E(J)$ traces for different values of applied strain, at fixed temperature and magnetic field, obtained for a bronze processed Nb_3Sn multifilamentary wire (sample 1).

surements. This current depends on the He gas pressure in the vacuum chamber and the temperature of the sample. Its record is useful in presetting the same experimental conditions for all the measurements under vacuum. Moreover, if a leak develops during the experiment, it can be directly detected by an increase of the heater-current.

The measurements are carried out as follows: the strain is set to the required value and the gear worm locked. Then the temperature of the sample is fixed and a magnetic field applied. The current through the sample is gradually increased and the voltage across the taps measured. $I-V$ traces are taken at different magnetic fields. The temperature is then incremented and $I-V$ measurements repeated as a function of field. Once the measurements at the required temperatures have been obtained, the strain is incremented and the procedure repeated. When the maximum strain ($\leqslant +0.7\%$) is reached, the strain is reduced and $I-V$ traces measured again to investigate the reversibility of J_c with strain. After returning to zero-strain, compressive strain can be applied as far as -0.7%. This cycle can be repeated if required.

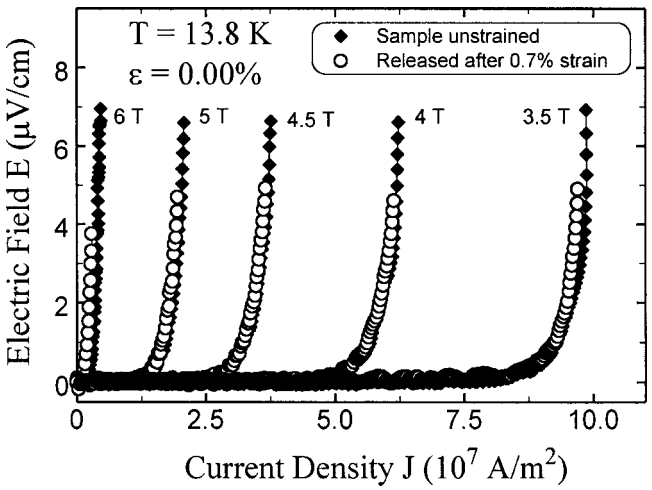

FIG. 6. $E(J)$ transitions for a bronze processed Nb_3Sn multifilamentary wire (sample 1), at different fields, that show the reversibility of J_c is independent of the electric field criterion.

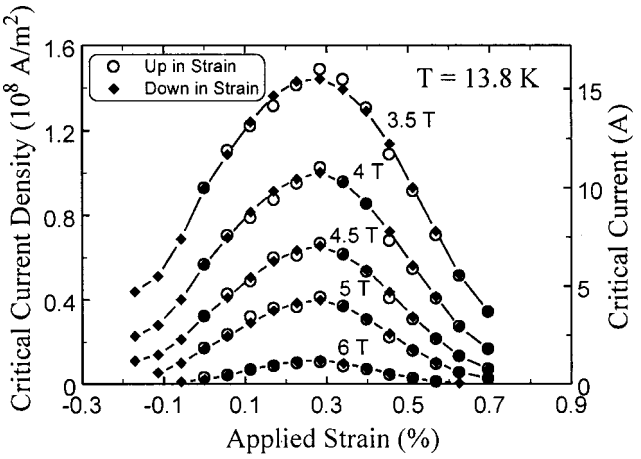

FIG. 7. $J_c(B,\varepsilon)$ data at 13.8 K using the 1μV/cm criterion, obtained for a bronze processed Nb_3Sn multifilamentary wire (sample 1). The results show the reversibility of J_c with applied strain.

VI. INVESTIGATION OF Nb_3Sn CONDUCTOR

To test the reliability of the probe, a bronze processed Vacuumschmelze Nb_3Sn multifilamentary wire was investigated. The sample was wound on a stainless steel mandrel and heat treated under an argon atmosphere at 700 °C for 64 h. It was then carefully transferred onto the spring and soldered to it. In this article, we present the results obtained on three samples from different parts of a single length of wire. For sample 1, the measurements were carried out at 9 and 13.8 K. The strain was incremented by $\Delta\varepsilon=0.057\%$ up to $+0.7\%$. At each value of applied strain, $I-V$ traces were taken at 9 and 13.8 K as a function of magnetic field up to 15 T. While releasing the strain, measurements were taken at 13.8 K to check the reversibility of J_c. After returning to zero strain, compressive strain was then applied with the same incremental change down to -0.17% and the measurements taken at 9 and 13.8 K. Sample 2 was investigated at 4.2 K from $+0.7$ % to -0.7 % to cover the whole range of strain. Finally, sample 3 was measured at 6.5 K, during two strain cycles between -0.23% and $+0.7\%$.

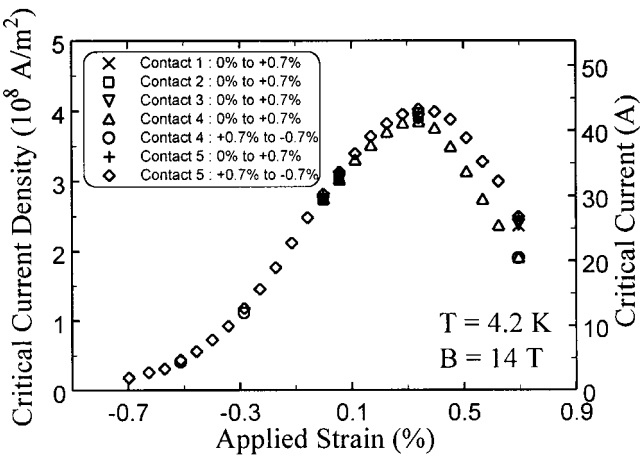

FIG. 8. $J_c(B,\varepsilon)$ data at 4.2 K, obtained for a bronze processed Nb_3Sn multifilamentary wire (sample 2) at five different positions of the sample. The results show that the mechanical properties are not uniform along the wire length.

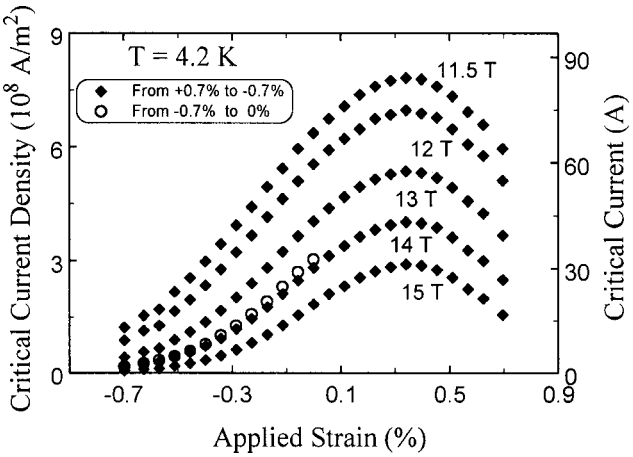

FIG. 9. $J_c(B,\varepsilon)$ data at 4.2 K, for strain values between +0.7% and −0.7%, obtained for a bronze processed Nb_3Sn multifilamentary wire (sample 2, contact 5).

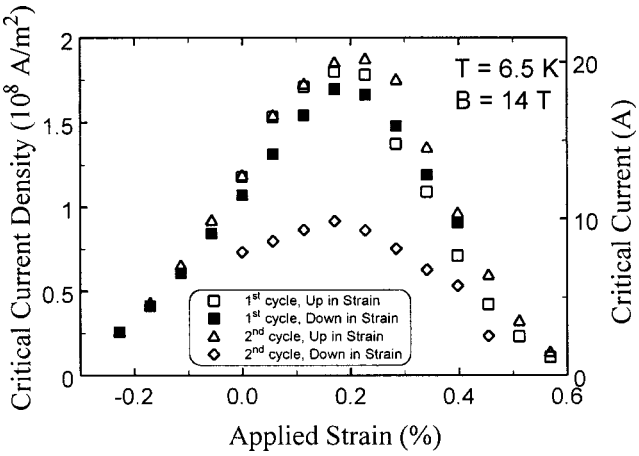

FIG. 10. $J_c(B,\varepsilon)$ data at 6.5 K, for two strain cycles between −0.23% and +0.7%, obtained for a bronze processed Nb_3Sn multifilamentary wire (sample 3).

VII. RESULTS

We have used an E-field criterion of 1 μV/cm to define J_c. Typical noise now achieved with screened external wiring is better than ±35 nV. Using the 1–2 cm gauge length for the voltage taps, an E-field criterion of 0.1 μV/cm for J_c can be measured. None of the results presented in this article are markedly dependent on which E-field criterion is chosen.

The results obtained for sample 1 are presented in Figs. 5–7. Typical examples of $E(J)$ traces, at fixed temperature and magnetic field, for different values of applied strain, are depicted in Fig. 5. Figure 6 presents $E(J)$ transitions at different fields, at 13.8 K, measured when the sample was unstrained and when it returned to zero strain after being strained up to +0.7%. It shows that the J_c remained reversible, independent of the electric field criterion used to define J_c. This result also reflects the good control of both strain and temperature achieved by the probe. Note that $E(J)$ transitions are quite steep in spite of the spring section being relatively thick, demonstrating that the electrical resistivity of the CuBe alloy is sufficiently high. Measurements above T_c show that the current through the shunt at 1μV/cm is as low as 60 mA.

The behavior of J_c with strain, at 13.8 K, is presented in Fig. 7 . The results obtained at 9 K are similar. At each field, J_c reaches a maximum value at a certain strain ε_m, originating from the precompression exerted on the Nb_3Sn filaments by the bronze matrix during the cooldown of the sample after the heat treatment. The strain value $\varepsilon_m(=0.26\%)$ is the same for both temperatures, and is in good agreement with the VAMAS program report.[39] Figure 7 also shows the reversibility of the J_c with strain. Details of these results are published elsewhere.[40]

Sample 2 was investigated at 4.2 K, throughout the strain window from +0.7% to −0.7%. The results are presented in Figs. 8 and 9 . The ability of the probe to investigate a wide range of strain, compressive as well as tensile, is clearly demonstrated. Five pairs of voltage taps were attached to the sample at different positions. Contact 1 and contact 5 were about half of a turn away from the spring ends. The three other contacts covered the middle two turns. The measurements were first taken at zero strain for the five pairs. The J_c varies by less than 1% (Fig. 8). One contact was chosen (contact 4) for detailed measurements of J_c as a function of strain (up to +0.7%) and magnetic field. The other four contacts were measured at 14 T, at 0%, 0.34%, and 0.7% strain. Apart from contact 4, all the other contacts show a good homogeneity and similar strain tolerance for J_c. The J_c of contact 4 shows similar behavior until the peak, but a significantly stronger dependence on strain from 0.34% to 0.7% as shown in Fig. 8. At $\varepsilon=+0.7\%$, another contact (contact 5) was measured in detail from +0.7% to −0.7% (results also presented in Fig. 9). The other contacts (including contact 4) were measured at 14 T, for a few values of strain. The J_c is reversible for the five contacts. At zero strain, the variation of J_c for all five contacts was less than 1.5%. This means that none of the contacts were damaged during the strain cycle. The behavior of contact 4 is different from the other contacts at high tensile strain regime. If this was due to variability of bending along the axis of the spring, it should have occurred in contact 3, which is situated in the middle of the spring turns. It rather shows that the mechanical properties are not uniform along the wire length. Irregularities in filaments diameter, sausaging, inhomogeneous distribution of filaments strength, as well as inhomogeneous distribution of voids may explain such differences. The peak position at $\varepsilon_m=0.34\%$, shifted as compared to the results of sample 1, may also originate from inhomogeneous mechanical properties along the wire.

The results obtained for sample 3 at 6.5 K are shown in Fig. 10. Sample 3 was first measured at 4.2 K as a function of strain up to +0.7% and back to zero strain. The value of ε_m is the same as for sample 1. The probe was then removed from the magnet cryostat to prepare it for measurements under vacuum. The measurements were then performed at 6.5 K, during two strain cycles between −0.23% and +0.7%. The position of ε_m moved to 0.20%. In contrast to sample 1 and sample 2, sample 3 did not show good reversibility of J_c with strain. Furthermore, J_c dropped dramatically, on average, by a factor of 2 during the second strain cycle from +0.7% to 0%. This behavior is probably due to the breakage of a fraction of Nb_3Sn filaments as a consequence of strain cycling.[31,32]

Sample 3 differed from sample 1 and sample 2 in that it was completely covered with a thick layer of solder (approximately 30 times the section of the wire). One can expect the mechanical properties of a large amount of solder to affect the behavior of Nb_3Sn wire by changing its deviatoric strain. Plastic deformation of the solder may cause the nonreversibility of J_c with strain. The results in Fig. 10 confirm that the amount of solder should be kept to a minimum. These results also demonstrate that the probe is suitable for studying the influence of fatigue on the transport properties of superconducting wires and tapes. Such studies are complementary to other investigations which address multiple cyclic loading (up to 10^7 cycles) at room temperature, prior to measurements at 4.2 K.[31–33]

VIII. DISCUSSION AND RECENT DEVELOPMENTS

An important general issue in making variable strain measurements is choosing whether or not to solder the wire or tape to a sample holder. In end-grip tensile measurements, the free standing sample is not soldered between the voltage taps so J_c can be measured directly in the strain-free state at 4.2 K.[2] If the sample is soldered to the sample holder (as in the work presented here), since the sample holder cannot be perfectly matched to the sample, there is inevitably some pre-strain on the sample after it has been cooled to 4.2 K. Although the pre-strain can be accounted for to first order by independently measuring the strain-free state of the wire, this requires a separate measurement. One has to balance the advantages of access to compressive measurements found by soldering samples against being unable to make a strain-free measurement directly. We are currently investigating the use of samples that are not soldered to the spring of the probe.[3]

Recently, the Cernox thermometer mounted next to the sample was calibrated as a function of field and temperature and used as the control thermometer. In addition, two Cernox thermometers have been installed at the ends of the sample and three independent heaters used to ensure uniform temperature along the sample. We installed thick brass current leads in the upper part of the probe[41] and thicker copper leads below the high vacuum current leadthroughs. Although this has increased the boil-off of the probe by about 50%, the range of critical current that can be measured has been extended. In liquid helium, critical currents in excess of 200 A have been measured at 4.2 K. From 6 to 16 K, the sample temperature is stable to ± 10 mK for currents up to 85 A.[42]

ACKNOWLEDGMENTS

The authors would like to thank C. R. Walters and E. Baynham at the Rutherford Laboratory for their valuable contribution. The authors acknowledge the excellent craftsmanship of G. Teasdale and P. Armstrong in the construction of the probe. The authors are grateful to Dr. D. Krus and I. Ringrose (Brush Wellman Inc.) for providing them with the technical data of CuBe alloy. The authors also thank P. A. Russell for her help in producing Figs. 1 and 2 of this article. This work is funded by the EPSRC (UK) GR/K70854 .

[1] E. Buehler and H. J. Levinstein, J. Appl. Phys. **36**, 3856 (1965).
[2] J. W. Ekin, Cryogenics **20**, 611 (1980).
[3] C. R. Walters, I. M. Davidson, and G. E. Tuck, Cryogenics **26**, 406 (1986).
[4] B. ten Haken, Ph.D. thesis, University of Twente, 1994.
[5] P. E. Richens, H. Jones, M. Van Cleemput, and D. P. Hampshire, IEEE Trans. Appl. Supercond. **7**, 1315 (1997).
[6] H. A. Hamid and D. P. Hampshire, Cryogenics **38**, 1007 (1998).
[7] J. W. Ekin, IEEE Trans. Magn. **MAG-17**, 658 (1981).
[8] J. W. Ekin, Adv. Cryog. Eng. **30**, 823 (1984).
[9] J. W. Ekin, D. K. Finnemore, Q. Li, J. Tenbrink, and W. Carter, Appl. Phys. Lett. **61**, 858 (1992).
[10] C. Park, D. P. Norton, J. D. Budai, D. K. Christen, D. Verebelyi, R. Feenstra, D. F. Lee, A. Goyal, D. M. Kroeger, and M. Paranthaman, Appl. Phys. Lett. **73**, 1904 (1998).
[11] J. W. Ekin, J. Appl. Phys. **49**, 3406 (1978).
[12] J. W. Ekin, A. F. Clark, and J. C. Ho, J. Appl. Phys. **49**, 3410 (1978).
[13] K. Ohmatsu, S. Hahakura, T. Kato, K. Fujino, K. Ohkura, and K. Sato, IEEE Trans. Appl. Supercond. **9**, 924 (1999).
[14] K. Watanabe, S. Awaji, M. Motokawa, Y. Mikami, J. Sakuraba, and K. Watazawa, Jpn. J. Appl. Phys., Part 2 **37**, L1148 (1998).
[15] D. M. Kroeger, D. S. Easton, C. C. Koch, and A. DasGupta, *Proceedings of the ICMC on Filamentary A15 Superconductors* (Plenum, New York, 1980), p. 205.
[16] B. ten Haken, A. Godeke, and H. H. J. ten Kate, J. Appl. Phys. **85**, 3247 (1999).
[17] C. M. Friend and D. P. Hampshire, Meas. Sci. Technol. **6**, 98 (1995).
[18] F. Mathu and H. C. Meijer, Cryogenics **22**, 428 (1982).
[19] N. J. Simon, E. S. Drexler, and R. P. Reed, *Properties of Copper and Copper Alloys at Cryogenic Temperatures* (The U.S. Government Printing Office, Washington, DC, 1992).
[20] S. J. S. Ford (Catalogue of Timet UK Limited, P.O. Box 704, Witton, Birmingham B6 7UR, UK) (private communication)..
[21] Metals Handbook, *Properties and Selection: Nonferrous Alloys and Pure Metals* 9th ed., Vol. 2 (American Society for Metals, Metals Park, OH, 1979).
[22] *Copper and Copper Alloy Springs* (Copper Development Association, 1944), Publication No. 39.
[23] B. ten Haken, T. N. Zaitseva, and H. H. J. ten Kate, Cryogenics **34**, 513 (1994).
[24] *Handbook of Chemistry and Physics*, 77th ed. (Chemical Rubber, Boca Raton, FL, 1996–1997).
[25] *Materials Properties Handbook-Titanium Alloys* (ASM International, 1994).
[26] *Materials at Low Temperatures*, edited by R. P. Reed and A. F. Clark (American Society for Metals, Metals Park, OH, 1983).
[27] A. F. Clark, G. Fujji, and M. A. Ranney, IEEE Trans. Magn. **MAG-17**, 2316 (1981).
[28] L. F. Goodrich, S. L. Bray, and T. C. Stauffer, Adv. Cryog. Eng. **36A**, 117 (1989).
[29] L. F. Goodrich and A. N. Srivastava, Cryogenics **35**, S29 (1995).
[30] H. Wada, C. R. Walters, L. F. Goodrich, and K. Tachikawa, Cryogenics **34**, 899 (1994).
[31] S. Ochiai and K. Osamura, Cryogenics **32**, 584 (1992).
[32] S. Ochiai, K. Osamura, and K. Watanabe, J. Appl. Phys. **74**, 440 (1993).
[33] S. Ochiai, T. Sawada, F. Sekino, M. Hojo, Y. Yamada, K. Takahashi, N. Ayai, and K. Watanabe, Semicond. Sci. Technol. **11**, 322 (1998).
[34] *Beryllium Copper* (Copper Development Association, 1958), Publication No. 54.
[35] Y. Kubo, F. Uchikawa, S. Utsunomiya, K. Noto, K. Katagiri, and N. Kobayashi, Cryogenics **33**, 883 (1993).
[36] H. Morita, K. Watanabe, K. Noto, K. Katagiri, R. Watanabe, and H. Fujimori, *Science Reports of the Research Institutes Töhoku University*, Series A: High-Field Superconductors, Vol. 37 (1992), p. 44.
[37] See, for example, J. Case and A. H. Chilver, *Strength of Materials and Structures* (Arnold, London, 1971).
[38] E. Oberg and F. D. Jones, *Machinery's Handbook*, 9th ed. (Industrial Press, New York, 1971).
[39] K. Katagiri, T. Okada, C. R. Walters, and J. W. Ekin, Cryogenics **35**, S85 (1995).
[40] N. Cheggour and D. P. Hampshire, J. Appl. Phys. **86**, 552 (1999).
[41] P. F. Hermann, *Current Leads. Handbook of Applied Superconductivity*, edited by B. Seeber (Institute of Physics, Bristol, 1998), p. 801.
[42] S. A. Keys and D. P. Hampshire (unpublished).